Article

Raman Spectra of Delignified Plant Fibers: Exploring the Impact of Xylan's Presence on Cellulose Spectral Features

Umesh Prasad Agarwal * and Sally A. Ralph

Posted Date: 29 November 2023

doi: 10.20944/preprints202311.1774.v1

Keywords: Lignocellulose; biomass; hemicellulose; FT-Raman spectroscopy

Article

Raman Spectra of Delignified Plant Fibers: Exploring the Impact of Xylan's Presence on Cellulose Spectral Features

Umesh P. Agarwal * and Sally A. Ralph

Fiber and Chemical Sciences Research, USDA FS, Forest Products Laboratory, 1 Gifford Pinchot Drive Madison, WI 53726-2398.

* Correspondence: umesh.p.agarwal@usda.gov; Tel.: (608) 231-9441

Abstract: Wood and plants are made of fibers which contain, in addition to cellulose, lignin and hemicelluloses. Xylan and galactoglucomannan are the dominant secondary cell wall hemicelluloses. Besides fibers' traditional use in textile and paper industries, the fibers are important materials for the biorefinery industry and for developing biocomposites. In the former context, renewable lignocellulosic biomass is used as feedstock to sustainably produce fuels, chemicals, and polymers. On the other hand, in relation to composites, cellulose fibers which are anisotropic play an important reinforcing role in fiber-matrix interactions. However, for these and other applications, structural analysis of the fibers is important and among many analytical techniques used, Raman spectroscopy is one of the methods. However, given the structural similarity between hemicelluloses and cellulose, many of their Raman contributions overlap. While the wavenumber positions corresponding to the Raman contributions of cellulose, hemicelluloses, and lignin are known, extent to which overlapping features of hemicellulose modify the spectrum of cellulose is not yet fully understood. The present investigation focuses on this aspect by using xylan as one of the hemicelluloses. As a model system, samples with various mass ratios of microcrystalline cellulose (cotton) and xylan (birch wood) were prepared and analyzed by FT-Raman spectroscopy. The findings were then applied to interpret Raman spectra of selected xylan containing delignified plant fibers. It is hoped that insights gained would lead to better interpretation of the spectra of natural and treated plant materials.

Keywords: lignocellulose; biomass; hemicellulose; FT-Raman spectroscopy

1. Introduction

Lignocellulosic biomass is an important feedstock that can serve as a sustainable raw material supply to produce chemicals, fuels, and biopolymers. In such biomass, after cellulose, hemicelluloses are the second most dominant component which are chemically heterogeneous in nature [1–3]. In many plant cells, xylan is one such structural polysaccharide composed of β-D-1,4-linked xylopyranosyl residues with numerous substitutions at C-2 and/or C-3 of the main chain by arabinose, galactose, glucuronic acid, and other monosaccharides [2]. It is found in the cell walls of land plants, in which it may constitute up to 30% of the dry weight. Nevertheless, its localization on cellulose fibers remains not well understood [4–8] and the presence of xylan seems to be one of the factors behind the low accessibility of cellulose [8,9]. In industrial applications, in the context of production of regenerated textile fibers where dissolving pulps are used, removal of hemicelluloses and particularly of xylan in hardwood pulps is important [9,10].

Raman spectroscopy is being increasingly used to analyze cellulose and lignocellulose materials [11–14]. It provides information on both the molecular composition and the molecular structure of cell walls. The technique is complementary to IR and offers several advantages. The Raman analysis is non-destructive, requires no sample preparation, and the presence of water in samples poses no problem. Additionally, there are many techniques available in Raman spectroscopy which can be used in the study of cellulose and lignocellulose materials. For example, to minimize sample fluorescence in the spectrum, FT- Raman spectroscopy is used where near-infrared (NIR) laser is used

 doi:10.20944/preprints202311.1774.v1

[15,16]. Another area has been the use of confocal Raman imaging where a sample can be chemically mapped at high spatial resolution [13,17,18]. Recently, reviews focusing on applications of Raman spectroscopy in plant biomass and cellulose materials have been published [14,18,19].

FT-Raman spectroscopy has been used to study wood and plant fibers and the spectral contributions of cellulose, hemicelluloses, and lignin are known [15,20], and it was concluded that the contributions of hemicellulose are broad and, in many regions, overlapped with those of cellulose [15]. One of the outcomes of the xylan's contribution at 1096 cm^{-1} was that the 380-Raman cellulose crystallinity of hemicellulose-containing materials was found to be lower compared to substances where the hemicellulose was absent or present in lower amounts [21]. Similarly, depending upon the sample composition, cellulose crystallinity data obtained by the other Raman methods may be affected [22,23]. Although in the Raman spectrum of black spruce wood, the contributions of glucomannan and xylan hemicelluloses were identified [15], how their presence modifies the spectral features of cellulose was not investigated. In this study, influence of xylan Raman contributions on the spectrum of crystalline cellulose is investigated by analyzing samples with various mixture compositions of crystalline cellulose and xylan. Subsequently, this knowledge is applied to better interpret Raman spectra of many delignified plant fibers that were mainly composed of cellulose and xylan.

2. Materials and Methods

Chemicals and materials. NaOH (AR grade) and sodium chlorite (technical grade) were obtained from Sigma–Aldrich (St. Louis, MO) or Alfa Aesar (Tewksbury, MA). Acetic acid glacial was from Fisher Scientific (Pittsburg, PA). Cotton MCC (microcrystalline cellulose), Whatman CC31 powder was from Whatman International Ltd., (Maidstone, UK). Birchwood xylan was purchased from Sigma–Aldrich (St. Louis, MO). All other chemicals and reagents, unless stated otherwise, were purchased from Sigma–Aldrich (St. Louis, MO). The samples of flax, aspen, willow, corn stalk, kenaf core, kenaf bast, and hardwood bleached kraft pulp (HWBKP) were available at the Forest Products Laboratory, Madison WI.

Cellulose-xylan mixture samples. Samples with various mixture compositions of crystalline cellulose and xylan were prepared by mixing cotton MCC (Whatman CC31) and xylan powders. In these mixtures MCC:xylan wt. ratios varied from 90:10 to 50:50. After physically mixing the samples, each sample was further mixed using few drops of methanol and was air dried at 25 °C before use.

Delignified samples. Wiley milled samples (40 mesh) of flax, aspen, willow, corn stalk, kenaf core, and kenaf bast were delignified by acid chlorite treatment. Acid chlorite treatment of the lignin-containing samples was carried out by using the previously reported method [21,24]. At about 70 °C, glacial acetic acid and sodium chlorite were added to the water-suspended samples, and the chemical charge was added three times over 7 h. The extent of delignification achieved was measured by the Klason method [25]. Data indicated that all samples were extensively delignified (Klason lignin 1–5%).

Chemical Composition Analysis. Selected lignocellulose samples were analyzed chemically to quantitate the amounts of Klason lignin [25] and carbohydrates [26]. Repeatability for Klason lignin was 0.4%, and for the carbohydrate analysis, the standard deviation was <1% [26].

FT-Raman spectroscopy. Samples were analyzed, in triplicate, with a Bruker MultiRam spectrometer (Bruker Instruments Inc., Billerica, MA). The Raman system is equipped with a 1,064-nm 1,000 mW continuous wave (CW) diode pumped Nd:YAG laser. Approximately 100 mg of each sample was pressed into a pellet with a hydraulic press. The laser power used for sample excitation was 600 mW and for each spectrum 2048 scans were accumulated. Bruker OPUS 7.2 software was used to determine peak positions and process the spectral data. The processing of spectra involved background removal, peak identification, and various mathematical operations. Background correction was performed using the "rubberband option" in OPUS using 64 baseline points. For plotting purposes, the spectra were converted to ASCII format which then allowed the spectral data to be exported to Excel.

 doi:10.20944/preprints202311.1774.v1

The quantitative analysis was carried out by measuring all samples under identical experimental conditions (same instrument, constant laser power, and scattering geometry). Additionally, toluene was used as an external standard because the ratio of analyte (cellulose or xylan) band intensity to external standard band intensity is proportional to analyte concentration and is independent of any changes in the experimental variables, e.g., laser power [27]. For each sample, the toluene spectra were measured before and after the sample analysis.

Raman band intensity and % band intensity changes. Intensities of various bands and changes in the intensities of selected Raman bands were calculated as follows. Using OPUS software, for 1480 and 1460 cm^{-1} peaks, a sloping line was drawn under each peak from 1440 to 1500 cm^{-1} and the peak heights were measured at 1480 and 1460 cm^{-1}. However, for the remaining cellulose peaks at 1121, 1096, 911, 898, 520, and 494 cm^{-1}, prior to measuring peak heights at the peak positions, a horizontal line under each peak was drawn, respectively, from 944, 944, 845, 845, 510, and 473 cm^{-1}. For the mixture samples, % band intensity changes were calculated using the following equation (Eq. 1).

$$\%\Delta I_{wavenumber} = [I_{wavenumber}\,(sample) - (x) * I_{wavenumber}(MCC)] * 100 \quad (1)$$

where $\Delta I_{wavenumber}$ is change in the band intensity at a selected wavenumber position in the sample spectrum and "x" is the faction of MCC present in that mixture-sample. For example, for a 60:40 mixture (60% MCC and 40% xylan), x would be 0.6 in Eq. 1.

3. Results and Discussion

3.1. Fiber Samples and Their Chemical Compositions

The chemical compositions of MCC and the delignified plant fibers are provided in Table 1. Considering that in Raman spectroscopy lignin can give rise to fluorescence and some of its spectral features overlap with that of cellulose [15,20], it was mostly removed by the mild acid chlorite delignification method [24]. In Table 1, the samples are listed in the order of high to low glucan content. In this investigation, fibers with high xylan content were chosen although its amount always remained less than 25% (Table 1). Moreover, except for delignified flax, the content of glucomannan in these materials was low (< 1.5%, Table 1). This was by design so that the spectral contributions of the latter would not further complicate the matter. None of the samples listed in Table 1 contain much lignin (in all cases < 4.5%) and residual proteins always showed up as Klason lignin due to its insolubility in the concentrated acid. The glucan content of the Table 1 materials varied between 92 and 45% and the cotton MCC was the most enriched in cellulose (> 90%). Of the xylan containing samples, except MCC and delignified flax, the rest had significant amount present (between 14 and 25%, Table 1).

Table 1. Chemical composition of cotton MCC and plant fibers.

Fiber samples	Glucan, %	Xylan, %	Mannan, %	Klason lignin,%	Ratio glucan:xylan[d]
Cotton MCC	92.2	0.1	ND[c]	3.1	99.9:0.1
Flax, delignified[a]	78.8	1.34	5.02	1.9	98.3:1.7
HWBKP[b]	73.8	14.8	ND	4.2	83.3:16.7
Kenaf core delignified	56.9	19.3	ND	2.1	74.7:25.3
Corn stalk, delignified	53.7	24.4	0.5	2.13	68.8:31.2
Willow, delignified	47.9	14.4	1.2	4.3	76.9:23.1
Aspen, delignified	44.6	16.7	1.4	3.3	72.8:27.2
Kenaf bast delignified	44.6	17.5	1.4	3.3	71.8:28.2

Preprints (www.preprints.org) | NOT PEER-REVIEWED | Posted: 29 November 2023 doi:10.20944/preprints202311.1774.v1

[a]After sample delignified by acid chlorite; [b]Hardwood bleached kraft pulp; [c]ND, not detected; [d]Assuming that the fibers are solely made of glucan and xylan (glucan + xylan = 100).

3.2. Raman Bands of Cellulose and Other Cell Wall Components

Raman spectra of MCC and xylan, in the fingerprint region, in the 250 to 1550 cm^{-1} are shown Figure 1. Additionally, below 250 cm^{-1}, only crystalline cellulose has bands at 172 and 93 cm^{-1} (not shown in Figure1). Table 2 lists the Raman bands of MCC as well as selected band wavenumbers of the other cell wall components (xylan, glucomannan, and lignin) [15,20]. For lignin, only those peak positions that overlap with the spectral features of crystalline cellulose are listed (Table 2). For each-component spectrum, the relative intensities of the bands, are designated in terms of very strong (vs), strong (s), medium (m), weak (w) etc. (Table 2). The spectral peak positions along with their assignments to the components are listed in Table 2.

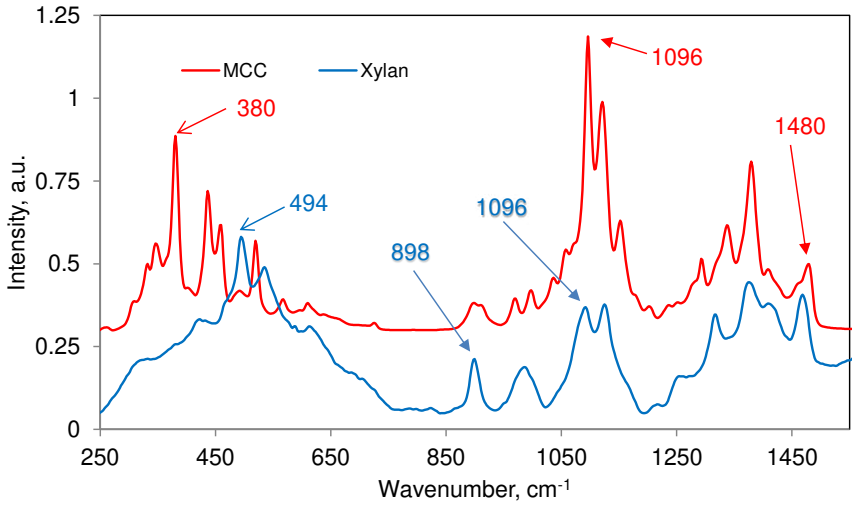

Figure 1. Raman spectra of MCC and xylan (250 – 1550 cm^{-1} region).

Table 2. Band positions of MCC and other cell wall components, 70 – 1550 cm^{-1} region.

Cellulose (MCC)	Xylan[a]	Glucomannan[a]	Lignin[b]	Comments
93 (m)[c]	—	—	—	Detected in only crystalline cellulose
172 (vw)	—	—	—	Detected in only crystalline cellulose
331 (w)	—	—	—	—
345 (w)	—	346 (w)	—	—
380 (m)	377(w)	—	384 (w)	Cellulose contribution dominates
437 (m)	—	—	—	—
459 (m)	—	—	463 (vw)	—
494 (w)	494(s)	492 (w)	491 (vw)	Xylan contribution dominates
520 (m)	—	—	522 (sh)	522 (sh) is only in syringyl lignins
567 (vw)	—	—	—	—
614 (vw)	614(m)	—	—	—
898 (m)	900(m)	897 (w)	895 (w)	Contributions mostly from MCC and xylan
911 (sh)	—	—	—	—
968 (w)	—	—	969 (vw)	—
998 (w)	—	—	—	—
1096 (s)	1091(s)	1089 (m)	1090 (w)	Order of contribution MCC > xylan > glucomannan >> lignin

Preprints (www.preprints.org) | NOT PEER-REVIEWED | Posted: 29 November 2023 doi:10.20944/preprints202311.1774.v1

1121 (s)	1126(s)	1121 (m)	1134 (m)	Order of contribution MCC > xylan > glucomannan > lignin
1152 (m)	—	—	—	—
1294 (m)	—	—	1297 (sh)	Both MCC and lignin contribute
1339 (m)	—	—	1333 (m)	Both MCC and lignin contribute
1380 (m)	1378(m)	1374 (m)	1363 (sh)	Order of contribution MCC > xylan = glucomannan
1409 (sh)	1413(m)	—		Both MCC and xylan contribute
1460 (sh)	—	1463 (m)	1454 (m)	Except xylan others contribute
1480 (m)	1469(m)	—	—	Both MCC and xylan contribute

[a]Reference [15]; [b]References [15,20]; [c]Relative band intensities in a spectrum are indicated by vs = very strong, s = strong, m = medium, w = weak, vw = very weak, and sh = shoulder.

3.3. Cellulose:Xylan Mixture Samples

Cellulose:xylan mixtures (respective ratio, 90:10 to 50:50; Table 3) were prepared and analyzed by Raman spectroscopy. Considering the mixture-spectra in Figure 2, the main bands of xylan (1469, 1126, 1091, 900, and 494 cm^{-1}, Table 2) overlapped with the cellulose features and modified their intensities to varying degrees. Therefore, for the mixture samples, peak intensity changes of the following 8 bands of cellulose were evaluated – 1480, 1460, 1121, 1096, 911, 898, 520, and 494 cm^{-1} (Figure 1, Table 2). Because the intensity change is sample-composition dependent, the percentage intensity change at a particular wavenumber (Table 3) was calculated using Eq. 1 where the actual fraction of MCC present was factored in. In Figure 3, the calculated band intensity changes are plotted against % xylan in the samples and, in most cases, good linear correlations (R^2 between 0.69 and 1.0) were obtained. This meant that the change in the xylan content accounted for the good amount of the variance in the MCC band intensities. However, 911 cm^{-1} band intensity showed poor correlation (R^2, 0.17, Figure 3) which may have to do with the fact that while both cellulose and xylan weakly contribute here (Table 2), only the falling wing of xylan's band at 900 cm^{-1} influences the intensity at 911 cm^{-1} (Table 2, Figure 1).

Table 3. Changes in MCC Raman band intensities as a function of xylan concentration.

Sample ID	**Xylan, %**	**MCC, %**	**Changes in selected MCC band intensities %***							
			ΔI_{1480}	**ΔI_{1460}**	**ΔI_{1121}**	**ΔI_{1096}**	**ΔI_{911}**	**ΔI_{898}**	**ΔI_{520}**	**ΔI_{494}**
MCC	0	100	NA	NA	NA	NA	NA	NA	NA	NA
Xylan	100	0	NA	NA	NA	NA	NA	NA	NA	NA
X1	10	90	-4.8	11.1	7.1	1.9	48.1	85.2	-25.9	122.2
X2	20	80	7.1	25.0	16.1	7.6	66.7	108.3	-37.5	275.0
X3	30	70	2.0	42.9	22.4	11.1	42.9	138.1	-28.6	471.4
X4	40	60	19.0	122.2	36.9	25.0	122.2	233.3	-16.7	733.3
X5	50	50	42.9	166.7	57.1	38.9	166.7	300.0	-33.3	1100.0

*Changes are with respect to pure MCC fraction present in the sample.

Preprints (www.preprints.org) | NOT PEER-REVIEWED | Posted: 29 November 2023 doi:10.20944/preprints202311.1774.v1

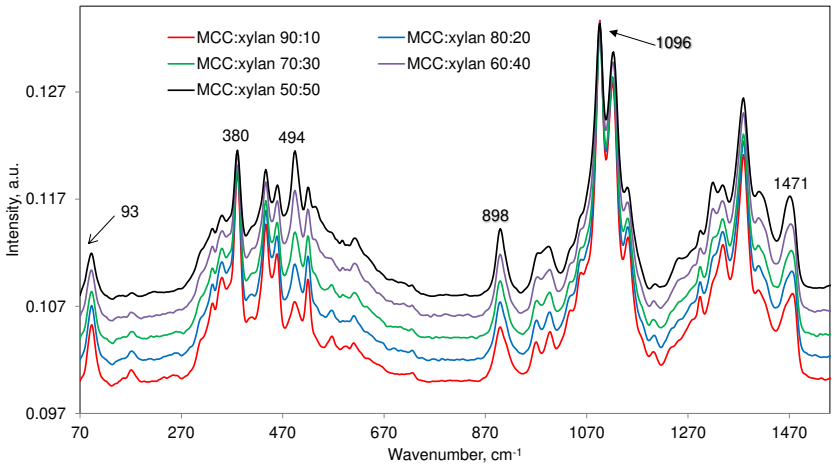

Figure 2. Raman spectra of mixture samples with various MCC: xylan mass ratios. Some of the peaks in the spectrum of mixture-sample (cellulose:xylan 50:50) are annotated.

With increased amount of xylan, while the intensities were greater at three locations (1460, 898, and 494 cm^{-1}, Figure 3), they declined at many other band locations (1480, 1121, 1096, and 520 cm^{-1}). All the latter being the wavenumber positions where MCC contributed strongly and, for 1121 and 1096 cm^{-1} bands, the implication was that any increased contribution from xylan (Table 2) was not enough to completely offset the decline caused by the reduction of MCC. A similar reduction was also noted for 520 cm^{-1} band because there was only minimal contribution from the nearby xylan peak at 494 cm^{-1} (Table 2, Figure 1) and therefore, for most of the samples, as the amount of cellulose in the sample declined so did the intensity at 520 cm^{-1} (Figs. 2 and 3).

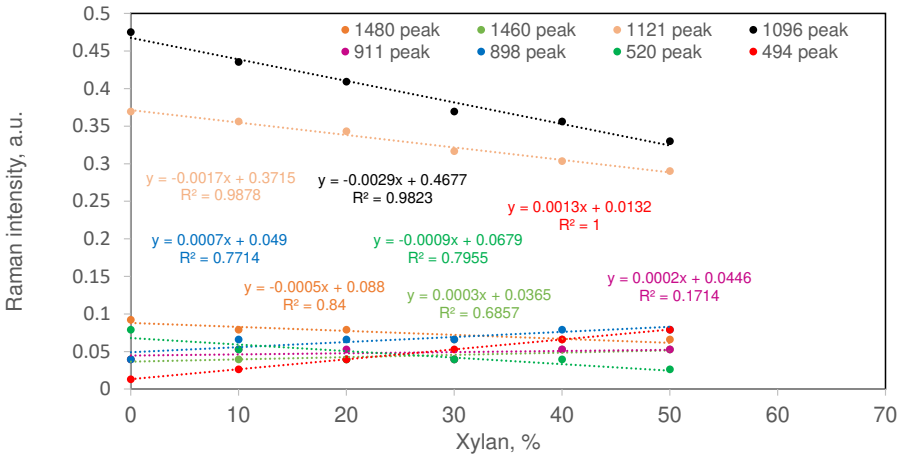

Figure 3. Band intensity changes in the Raman spectra of the various MCC: xylan mixture-samples.

The results of the percent intensity changes with respect to cellulose fraction in the mixture ($\%\Delta I_{wavenumber}$, Eq.1) are reported in Table 3. From this data, clearly, when the band intensities of pure MCC at the fractions that existed in the mixtures (e.g., sample X4 in Table 3, x = 0.6 sample MCC fraction 60%) were compared with their Raman intensities in the mixtures, for most of the MCC bands, the mixture-intensities increased and such increases correlated well with the xylan amounts in the mixtures (Table 3, R^2 between 0.97 and 0.75 - Figure 4). For instance, $\% \Delta I_{1460}$ increased from 11% to 167% (Table 3, samples X1 to X5). In contrast, 520 cm^{-1} MCC peak showed a decline upon increase in xylan content (Figure 4). Based on data in Table 3, most decline occurred for sample X2 (xylan:MCC 20:80). This result can be rationalized as follows. Because of xylan being additionally present in the mixtures, the 520 and 494 cm^{-1} peaks overlapped in a way that made the calculation of

Preprints (www.preprints.org) | NOT PEER-REVIEWED | Posted: 29 November 2023 doi:10.20944/preprints202311.1774.v1

the former's peak height less accurate (as described in Materials and Methods, a horizontal baseline under the band was drawn from 510 cm^{-1}) (Figure 1; Table 3). On the other hand, due to xylan's Raman contributions, the rest of the MCC band intensities increased to various degrees (Table 3, Figure 4). In summary, based on Figure 4, the order of the intensity changes (%) was as follows – $\Delta I_{494} > \Delta I_{898} > \Delta I_{911} > \Delta I_{1460} > \Delta I_{1480}$. Later, for fiber samples, this information would be used to understand how xylan impacts the spectral intensities of cellulose.

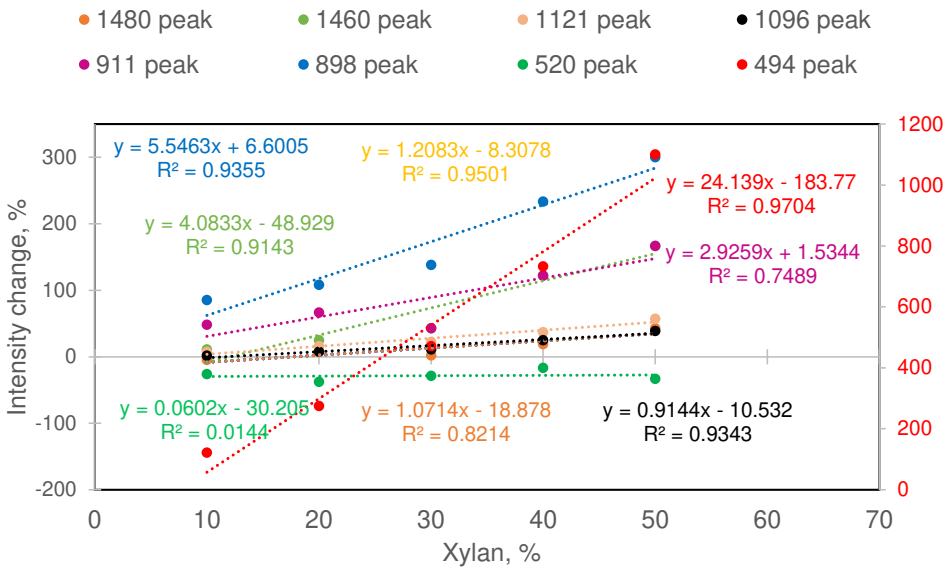

Figure 4. Intensity changes (%) in MCC bands with respect to its fractions in various mixture samples.

The other point to note is that in the region where the spectral features of the sample components significantly overlap the band position of the mixture-sample can undergo a shift. Usually, the shift depends upon both the initial intensities of the bands involved and the sample composition. This is illustrated in Figure 5 where 1400 to 1500 cm^{-1} region spectra of various mixture-samples along with those of the two components (MCC and xylan) are shown. As can be noted, due to the band overlap, the pure MCC peak, originally located at 1480 cm^{-1} shifted to lower wavenumbers. In the case of cellulose:xylan 50:50 sample, the peak shifted by 8 cm^{-1}.

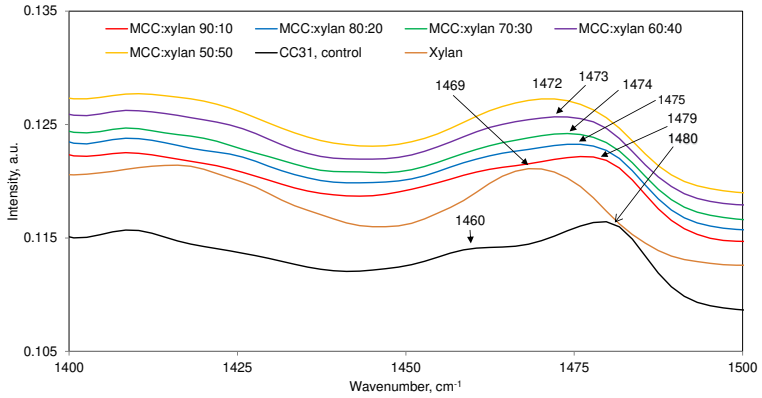

Figure 5. Band positions of the different composition samples in the region 1450 -1500 cm^{-1}.

Preprints (www.preprints.org) | NOT PEER-REVIEWED | Posted: 29 November 2023 doi:10.20944/preprints202311.1774.v1

Another example of band-overlap is seen in 900 cm^{-1} region where MCC has two peaks (898 and 911 cm^{-1}, Figure 6) and xylan only one at 898 cm^{-1}. Although at low xylan level (e.g., MCC:xylan 80:20 sample) the MCC shoulder at 911 cm^{-1} is still perceptible, it fades at higher xylan levels (Figure 6). Moreover, contrary to the 1450 – 1550 cm^{-1} region situation that was discussed above, no significant shift of 898 cm^{-1} MCC peak is observed because this peak is common to both MCC and xylan, and the MCC feature at 911 cm^{-1} is quite weak.

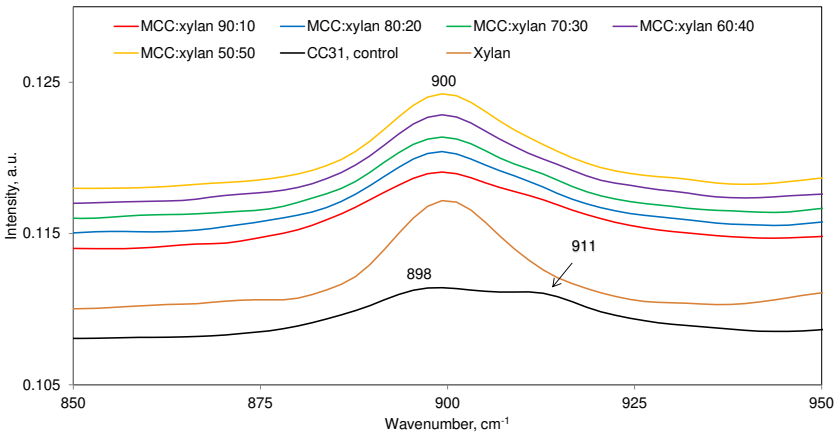

Figure 6. Band profiles of the mixture-samples and their components (MCC and xylan) in 900 cm^{-1} region.

4. Applications to Fibers

Raman spectra of fibers were obtained under identical conditions and corrected by using an external standard (toluene). Therefore, the obtained band intensities can be compared directly. In Figure 7, spectra of the two delignified plant fibers (flax and aspen) and MCC are compared. Moreover, band intensities for these and other fiber samples are listed in Table 4. The intensities are not normalized for the differing content of glucan in the fibers (Table 1). When the data for MCC, flax, and aspen are compared (Tables 1 and 4, Figure 7), Raman features of MCC were found to be highly resolved and significantly more intense (e.g., compare band intensities I_{1480}, I_{1121}, I_{1096}, and I_{520}, Table 4). Even after accounting for the glucan-content differences between them, the MCC band intensities remained higher (Tables 1 and 4). Moreover, this holds true even when the xylan contributions are present in the spectra (xylan's presence makes many of these intensities higher). This is because unlike MCC plant-cellulose is significantly less crystalline. Therefore, in the following, for appraising the fibers' spectra for contributions of xylan, instead of MCC, spectral data of delignified flax (which has 79% cellulose and 98.3:1.7 glucan:xylan ratio, Table 1) would be used.

Table 4. Raman intensities of selected bands.

Sample ID	Band intensities[a], a.u.							
	I_{1480}	I_{1460}	I_{1121}	I_{1096}	I_{911}	I_{898}	I_{520}	I_{494}
Cotton MCC	0.157	0.07	0.673	0.871	0.074	0.081	0.156	0.031
Flax, delignified	0.041	0.027	0.202	0.248	0.027	0.034	0.024	0.007
HWBKP	0.05	0.041	0.291	0.335	0.04	0.068	-0.02	0.038
Kenaf core, delignified	0.038	0.063	0.215	0.234	0.039	0.061	0.019	0.023
Corn stalk, delignified	0.04	0.053	0.274	0.289	0.047	0.073	0.021	0.039
Willow, delignified	0.053	0.069	0.319	0.359	0.048	0.075	0.015	0.032
Aspen, delignified	0.04	0.053	0.274	0.289	0.047	0.073	0.021	0.039
Kenaf bast, delignified	0.047	0.070	0.247	0.275	0.04	0.059	0.028	0.022

[a]Not normalized for different cellulose contents.

Preprints (www.preprints.org) | NOT PEER-REVIEWED | Posted: 29 November 2023 doi:10.20944/preprints202311.1774.v1

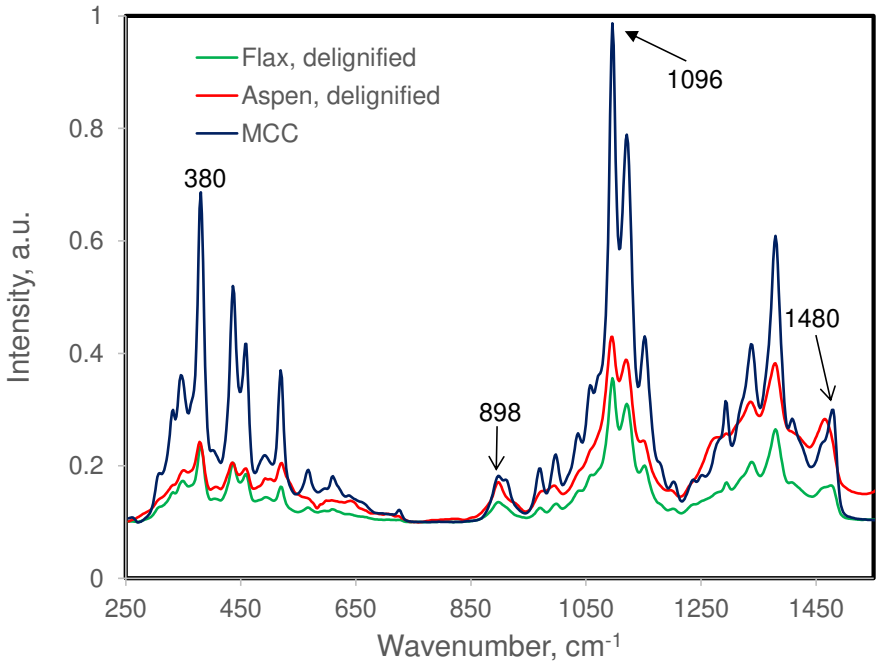

Figure 7. Raman spectra of MCC, delignified aspen, and delignified flax.

Comparing Band Intensities

Considering the Table 4 intensity data, for the non-MCC samples, I_{1480} data are similar and small variation among the low and high-xylan samples (Table 1) can be understood in terms of a) xylan contributions at 1480 cm^{-1} (Figure 5) and b), in higher cellulose samples, greater contribution coming from cellulose (i.e., delignified flax and HWBKP, Tables 1 and 4). Next, considering I_{1460} data, the intensities for flax and HWBKP were lower compared with the rest of the fiber samples. This is likely to be because between the two bands of MCC at 1480 and 1460 cm^{-1}, the latter is significantly weaker (Figure 5) and even though these two samples have higher amount of cellulose this does not fully compensate for the lower amount of xylan, which also contributes here (Figure 5). However, in the rest of the fiber-samples, compared to flax, xylan's contribution at 1460 cm^{-1} is higher. In contrast, in the fibers, the Raman intensities I_{1121} and I_{1096} did not vary all that much and therefore, at these wavenumbers the contributions from cellulose dominated. The other bands in the fibers' spectra (Figure 8) that showed higher Raman intensities when significant amount of xylan was present were 911, 898 and 494 cm^{-1} (Table 4). Compared to delignified flax (1.34% xylan, Table 1), the I_{911}, I_{898}, and I_{494} were higher, respectively, by at least 1.5, 1.7, and 3 times (Table 4). As mentioned above, such increases are in accordance with the prediction ($\Delta I_{494} > \Delta I_{898} > \Delta I_{911} > \Delta I_{1460} > \Delta I_{1480}$, Table 3) that was based upon the analysis of the MCC and xylan mixtures (Figure 4). The highest increase was observed at 494 cm^{-1} (Figure 9, Table 4) in accordance with the expectation that in the Raman spectrum of xylan this is one of the strongest peaks (Figure 1, Table 2).

Preprints (www.preprints.org) | NOT PEER-REVIEWED | Posted: 29 November 2023 doi:10.20944/preprints202311.1774.v1

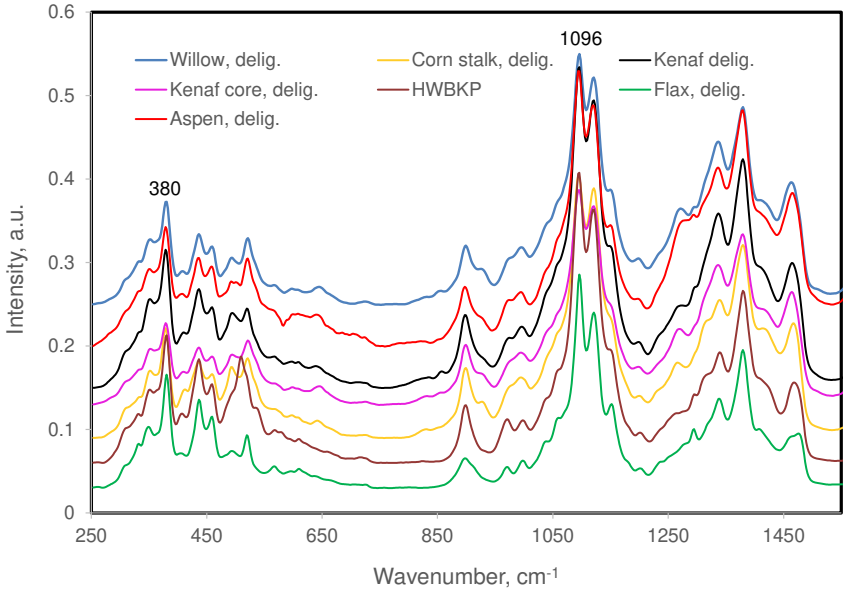

Figure 8. Raman spectra of various plant fibers.

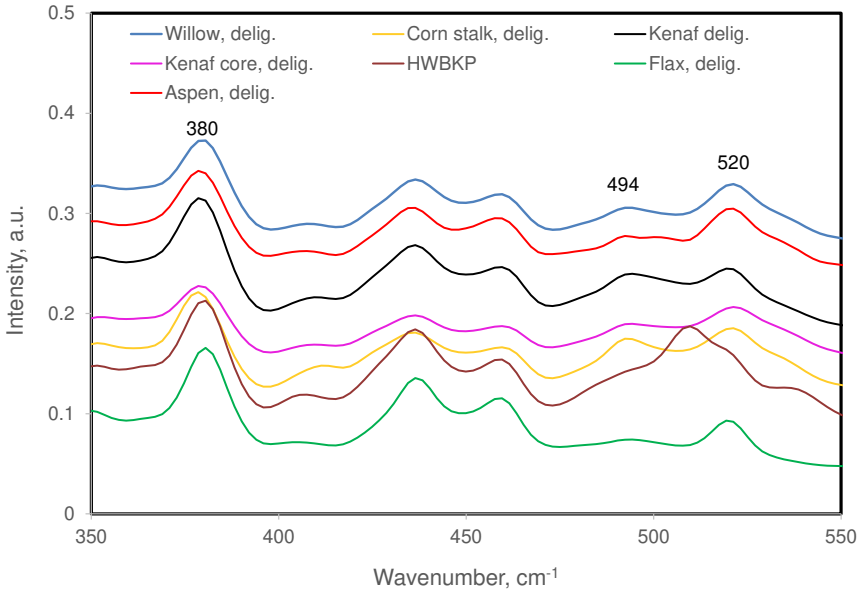

Figure 9. Raman spectra of plant fibers: comparison of 494 cm^{-1} band due to xylan.

5. Conclusions

To better understand Raman spectra for plant fibers and other cellulosic biomass, spectra of samples made from the mixture of microcrystalline cellulose (MCC) and xylan were investigated. It was found that in spectral regions where contributions of both MCC and xylan were present, the cellulose spectrum was modified significantly. Such modifications depended on the compositions of the mixture-samples as well as on the band intensities of the overlapping spectral features of the components. This information was then used to interpret spectra of xylan containing wood and plant fibers and it was shown that the most affected cellulose peaks were 1480, 1460, 911, 898, and 494 cm^{-1}. It is hoped that insights obtained will be useful in better interpretation of spectra of plant materials.

Author Contributions: Author contributions: U.P.A. carried out conceptualization, methodology, and all the analysis work. He also wrote the entire manuscript. S.R. carried out many of the experiments and reviewed the manuscript draft. **B**oth authors have read and agreed to the published version of the manuscript.

Funding: No external funding was received for carrying out this study.

Conflicts of Interest: The authors declare no competing financial interest.

References

1. Han, J.S.; Rowell, J.S. Chemical Composition of Fibers In: *Paper and Composites from Agro-based Resources*. Eds., R.M. Rowell, R.A. Young, and J.K. Rowell. CRC Press Inc., Boca Raton, FL. 1997; pp 83-134.
2. Albersheim, P.; Darvill, A.; Roberts, K.; Sederof, R.; Staehelin, A. Plant cell walls: from chemistry to biology, 1st Edn. Garland Science, New York. 2010.
3. Terrett, O.M.; Dupree, P. Covalent interactions between lignin and hemicelluloses in plant secondary cell walls. *Curr. Opin. Biotechnol.* **2019**, 56, 97–104. https://doi.org/10.1016/j.copbio.2018.10.010
4. Park, Y.B.; Cosgrove, D.J. Xyloglucan and its interactions with other components of the growing cell wall. *Plant Cell Physiol.* **2015**, 56, 180–194; https://doi.org/10.1093/pcp/pcu204.
5. Berglund, J.; Mikkelsen, D.; Flanagan, B.M.; Dhital, S.; Gaunitz, S.; Henriksson, G.; Lindström, M.E.; Yakubov, G.E.; Gidley, M.J.; Francisco Vilaplana, F. Wood hemicelluloses exert distinct biomechanical contributions to cellulose fibrillar networks. *Nat. Commun.* **2020**, 11, 4692. https://doi.org/10.1038/s41467-020-18390-z
6. Salmén, L. On the organization of hemicelluloses in the wood cell wall. *Cellulose* **2022**, 29,1349–1355. https://doi.org/10.1007/s10570-022-04425-9
7. Terrett, O.M.; Lyczakowski, J.J.; Yu, L.; Iuga, D.; Franks, W.T. Brown, S.P.; Dupree, R.; Dupree, P. Molecular architecture of softwood revealed by solid-state NMR. *Nat. Commun.* **2019**, 10, 4978. https://doi.org/10.1038/s41467-019-12979-9.
8. Pękala, P.; Szymańska-Chargot, M.; Zdunek, A. Interactions between non-cellulosic plant cell wall polysaccharides and cellulose emerging from adsorption studies. *Cellulose* **2023**, 30, 9221–9239. https://doi.org/10.1007/s10570-023-05442-y
9. Spönla, E.; Rahikainen, J.; Potthast, A.; Grönqvist, S. High consistency enzymatic pretreatment of eucalyptus and softwood kraft fibres for regenerated fibre products. *Cellulose* **2023**, 30, 4609–4622. https://doi.org/10.1007/s10570-023-05144-5
10. Wollboldt, R.P.; Zuckersta¨tter, G.; Weber, H.K. Larsson, P.T.; Sixta, H. Accessibility, reactivity, and supramolecular structure of E. globulus pulps with reduced xylan content. *Wood Sci. Technol.* **2010**, 44, 533–546. https://doi.org/10.1007/s00226-010-0370-2
11. Agarwal, U.P. 1064 nm FT-Raman spectroscopy for investigations of plant cell walls and other biomass materials. *Front. Plant Sci.* **2014**, 5: 490; https://doi.org/10.3389/fpls.2014.00490
12. Lupoi, J.S.; Singh, S.; Simmons, B.A.; Henry, R.J. Assessment of Lignocellulosic Biomass Using Analytical Spectroscopy: An Evolution to High-Throughput Techniques. 2014, 7, 1–23. https://doi.org/10.1007/s12155-013-9352-1
13. Gierlinger, N. New Insights into Plant Cell Walls by Vibrational Microspectroscopy. *Appl. Spectrosc. Rev.* **2018**, 53, 517–551. https://doi.org/10.1080/05704928.2017.1363052
14. Agarwal, U.P. Analysis of Cellulose and Lignocellulose Materials by Raman Spectroscopy: A Review of the Current Status. *Molecules* **2019**, 24, 1659. https://doi.org/10.3390/molecules24091659
15. Agarwal, U.P.; Ralph, S.A. FT-Raman Spectroscopy of Wood: Identifying contributions of lignin and carbohydrate polymers in the spectrum of black spruce (Picea mariana). *Appl. Spectrosc.* **1997**, 51, 1648–1655; https://doi.org/10.1366/00037029719393
16. Himmelsbach, D.S.; Akin, D.E. Near-Infrared Fourier-Transform Raman Spectroscopy of Flax (Linum usitatissimum L.) Stems. *J. Agric. Food Chem.* **1998**, 46, 991–998. https://doi.org/10.1021/jf970656k
17. Agarwal, U.P. Raman imaging to investigate ultrastructure and composition of plant cell walls: distribution of lignin and cellulose in black spruce wood (*Picea mariana*). *Planta* **2006**, 224: 1141–1153; https://doi.org/10.1007/s00425-006-0295-z
18. Kanbayashi, T.; Kataoka, Y.; Ishikawa, A.; Matsunaga, M.; Kobayashi, M.; Kiguchi, M. Depth profiling of photodegraded wood surfaces by confocal Raman microscopy. *J. Wood Sci.* **2018**, 64, 169. https://doi.org/10.1007/s10086-018-1698-8
19. Saletnik, A.; Saletnik, B.; Puchalski, C. Overview of popular techniques of Raman spectroscopy and their potential in the study of plant tissues. *Molecules* **2021**, 26, 1537. https://doi.org/10.3390/molecules26061537
20. Agarwal, U.P.; McSweeny, J.D.; Ralph, S.A. FT–Raman Investigation of Milled-wood Lignins: Softwood, hardwood, and chemically modified black spruce lignins. *J. Wood Chem. Technol.* **2011**, 17, 324–344. https://doi.org/10.1080/02773813.2011.562338

21. Agarwal, U.P.; Reiner, R.S.; and Ralph, S.A. Estimation of cellulose crystallinity of lignocelluloses using near-IR FT-Raman spectroscopy and comparison of the Raman and Segal-WAXS methods. *J. Agric. Food Chem.* **2013**, 61, 103–113. https://doi.org/10.1021/jf304465k
22. Schenzel, K.; Fischer, S.; Brendler, E. New method for determining the degree of cellulose I crystallinity by means of FT Raman spectroscopy. *Cellulose* 2005, **12**, 223–231.
23. Agarwal, U.P; Ralph, S.A.; Reiner, R.S.; Baez, C. New cellulose crystallinity estimation method that differentiates between organized and crystalline phases. *Carbohydr. Poly.* 2018, **190**, 262–270. https://doi.org/10.1016/j.carbpol.2018.03.003
24. Browning, B. L. Methods of Wood Chemistry; Wiley-Interscience:New York, 1967; Vol. II.
25. TAPPI Test Method. Acid insoluble lignin in wood and pulp; official test method T-222 (Om). 1983, TAPPI, Atlanta.
26. Davis, M.W. A rapid method for compositional carbohydrate analysis of lignocellulosics by high pH anion-exchange chromatography with pulse amperometric detection (HPAE/PAD). *J. Wood Chem. Technol.* **1998**, 18, 235–252. https://doi.org/10.1080/02773819809349579
27. Pelletier, M.J. Quantitative Analysis Using Raman Spectrometry. *Applied Spectrosc.* **2003**, 57, 20A–42A. https://doi.org/10.1366/0003702033211651